

## Performance Analysis of Spectrum Sharing Systems with Distributed CDD

Kim, K.J.; Liu, H.; Di Renzo, M.; Poor, H.V.

TR2018-162 December 07, 2018

### Abstract

In this paper, a cooperative spectrum sharing system is investigated. To effectively access the radio spectrum licensed to the primary users, the distributed cyclic delay diversity (dCDD) scheme is employed as the transmit diversity scheme for distributed cyclic-prefixed single carrier transmissions. As a setup for the secondary users' network, it is assumed that it comprises the control unit and a group of remote radio heads. In the secondary users' network, a single primary user transmitter is assumed to be located isotropically, so that a mixture of line-ofsight and non-line-of-sight paths over frequency selective fading channels is considered. One of the objectives of this paper is to investigate the effects of this new channel model on the outage probability promised by dCDD. A closedform expression for the outage probability is derived first, and then its asymptotic expression is derived to characterize the maximum achievable diversity gain. Link-level simulations are also conducted to verify the performance analysis.

*IEEE Global Communications Conference (GLOBECOM)*

This work may not be copied or reproduced in whole or in part for any commercial purpose. Permission to copy in whole or in part without payment of fee is granted for nonprofit educational and research purposes provided that all such whole or partial copies include the following: a notice that such copying is by permission of Mitsubishi Electric Research Laboratories, Inc.; an acknowledgment of the authors and individual contributions to the work; and all applicable portions of the copyright notice. Copying, reproduction, or republishing for any other purpose shall require a license with payment of fee to Mitsubishi Electric Research Laboratories, Inc. All rights reserved.



# Performance Analysis of Spectrum Sharing Systems with Distributed CDD

Kyeong Jin Kim\*, Hongwu Liu†, Marco Di Renzo‡, and H. Vincent Poor§

\*Mitsubishi Electric Research Laboratories (MERL), Cambridge, MA, USA

†Shandong Jiaotong University, Jinan 250357, China

‡Laboratoire des Signaux et Systèmes, CNRS, CentraleSupélec, Univ Paris Sud

Université Paris-Saclay, 3 rue Joliot Curie, Plateau du Moulon, 91192, Gif-sur-Yvette, France

§Department of Electrical Engineering, Princeton University, Princeton, NJ, USA

**Abstract**—In this paper, a cooperative spectrum sharing system is investigated. To effectively access the radio spectrum licensed to the primary users, the distributed cyclic delay diversity (dCDD) scheme is employed as the transmit diversity scheme for distributed cyclic-prefixed single carrier transmissions. As a setup for the secondary users’ network, it is assumed that it comprises the control unit and a group of remote radio heads. In the secondary users’ network, a single primary user transmitter is assumed to be located isotropically, so that a mixture of line-of-sight and non-line-of-sight paths over frequency selective fading channels is considered. One of the objectives of this paper is to investigate the effects of this new channel model on the outage probability promised by dCDD. A closed-form expression for the outage probability is derived first, and then its asymptotic expression is derived to characterize the maximum achievable diversity gain. Link-level simulations are also conducted to verify the performance analysis.

**Index Terms**—Distributed CDD, spectrum sharing, cyclic-prefixed single carrier transmission, outage probability, diversity gain.

## I. INTRODUCTION

Maximum ratio transmission (MRT) was proposed as a transmit diversity scheme by [1] for a transmitter equipped with multiple antennas. Recently, MRT has been applied to the distributed system [2]. However, acquiring exact channel state information (CSI) at the transmitter side is a challenging task in distributed wireless communications systems that apply the transmit diversity scheme. As an alternative scheme, transmit antenna selection (TAS) has been proposed by [3]–[5], when multiple antennas are deployed at the transmitter. Considering feedback overhead and signal processing cost, a single transmit antenna is selected in TAS to maximize the signal-to-noise ratio (SNR) at the secondary user receiver (SRX). In addition, a general maximal ratio combining (MRC) is applied among several receiver antennas to enhance the performance of the secondary users’ network.

In contrast to MRT and TAS, distributed cyclic delay diversity (dCDD) has been proposed as a practical transmit diversity scheme for cyclic-prefixed single carrier (CP-SC)

This work was supported in part by the U.S. National Science Foundation under Grants CNS-1702808 and ECCS-1647198. The work of Marco Di Renzo was supported in part by the European Commission through the H2020-MSCA ETN-5Gaura project under Grant Agreement 675806.

systems [6]. Without explicit channel feedback from the receiver side, dCDD improves the reliability of a message by transmitting the same message over multiple channels having different channel characteristics. Several works [7]–[10] have applied the conventional cyclic delay diversity (CDD) for several applications. In contrast to the conventional CDD, which applies a cyclic delay among antennas deployed at the same transmitter, dCDD applies a cyclic delay among antennas, each of which is deployed at a different transmitter. By proper design of the permutation matrix that circularly shifts the symbol block, an intersymbol interference (ISI)-free channel matrix can be generated. The size of the symbol block and the maximum number of multipath components of the channel that transmits this symbol block determine the number of transmitters for dCDD. It has been verified by [6] that the full diversity gain with a higher coding gain can be achieved over those of [3]–[5] and [11]–[13] without exact knowledge of CSI at the transmitter side. This performance gain advantage will be beneficial to secondary users in reusing the radio spectrum licensed to primary users.

There are several existing works, e.g. [12], [13] that consider spectrum sharing systems that use CP-SC transmissions. In contrast to these existing works, we can summarize our main contributions as follows.

- To achieve the transmit diversity gain, dCDD is employed between the control unit (CU) and a finite number of secondary user remote radio heads (SU-RRHs). We use a mathematical analysis fit to finite-sized cooperative spectrum sharing systems. For a secondary users’ network, we investigate the impact of the isotropic random location of the primary user transmitter (PTX) on the outage probability. Thus, the use of dCDD in the spectrum sharing system is one of the key distinctions from [12], [13].
- Due to the random location of the PTX within the secondary users’ network, a more practical channel model, which is somewhat similar to that of [14]–[17], is used. The co-existence of line-of-sight (LoS) and non-line-of-sight (nLoS) paths is modeled by using a time-sharing factor [18], which is distributed according to a Bernoulli

process.

- We provide an analytical framework jointly taking into account a different degree of remote radio head (RRH) cooperation via dCDD, frequency selective fading, and isotropic random location of the PTX over the co-existing LoS and nLoS paths. For this new setting for the spectrum sharing system, a new expression for the spatially averaged signal-to-interference ratio (SA-SIR) is derived.
- We analyze the achievable diversity gain from the outage probability.

### A. Notation

$\mathbb{C}$  denotes the set of complex numbers;  $\mathcal{CN}(\mu, \sigma^2)$  denotes the circularly symmetric complex Gaussian distribution with mean  $\mu$  and variance  $\sigma^2$ ;  $F_\varphi(\cdot)$  and  $f_\varphi(\cdot)$ , respectively, denote the cumulative distribution function (CDF) and probability density function (PDF) of the random variable (RV)  $\varphi$ ;  $E\{\cdot\}$  denotes expectation. The length of a vector  $a$  is denoted by  $\mathbb{L}(a)$ .

## II. SYSTEM AND CHANNEL MODELS

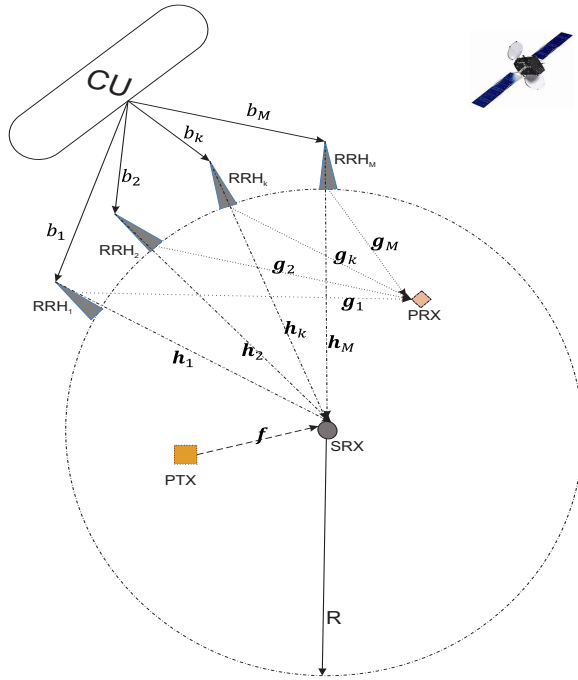


Fig. 1. Illustration of the considered dCDD-based spectrum sharing system with the PTX placed at random within the secondary user's cell.

Fig. 1 illustrates the considered dCDD-based spectrum sharing system comprising one PTX and primary user receiver (PRX) in the primary licensed frequency band. A disk-shaped communication cell of radius  $R$  for the secondary users is formed around the SRX. In the cell, the location of the PTX is assumed to be isotropic, whereas the PRX is placed at a fixed location. A group of secondary SU-RRHs are distributed over the circumference of the cell. A secondary user network consisting of the CU,  $M$  SU-RRHs, and SRX shares the primary users' licensed frequency band subject to interference

constraints imposed by the PRX. The CU controls  $M$  single antenna equipped RRHs,  $\{\text{RRH}_m\}_{m=1}^M$ , via dedicated highly reliable backhauls,  $\{b_m\}_{m=1}^M$ . The CU forms an information signal to be transmitted by SU-RRHs simultaneously to the SRX by using dCDD, so that each SU-RRH requires only simple hardware and low transmission power in communicating with the SRX. A receiving unit for a Global Navigation Satellite System (GNSS) signal is installed at the front-end of each node, so that SU-RRHs can receive and transmit the same information at the same time when they are operating for dCDD. Due to the use of half-duplex transceivers in all nodes, they are allowed to either send or receive data at any given time.

Since the number of SU-RRHs for dCDD is limited by the symbol block size and the maximum multipath path components over the frequency fading channel in the secondary users' network [6], this paper investigates only a finite-sized cooperative spectrum sharing system comprising a finite number of SU-RRHs for dCDD and a single SRX. By employing appropriate channel sounding scheme or channel reciprocity [19], [20], we further assume that the SRX is able to know the maximum number of multipath components over the channels from SU-RRHs to itself. The following channels are assumed in the considered system.

- Channels from SU-RRHs to the SRX: A multipath channel,  $\mathbf{h}_m$ , from the  $m$ th SU-RRH to the SRX is given by

$$\mathbf{h}_m = \sqrt{R^{-\epsilon_L}} \tilde{\mathbf{h}}_m \quad (1)$$

where  $\tilde{\mathbf{h}}_m$  denotes a frequency selective fading channel with  $N_h \triangleq \{\mathbb{L}(\tilde{\mathbf{h}}_m)\}_{m=1}^M$  multipath components, and  $\epsilon_L$  denoting the path loss exponent of all the LoS paths over all  $\{\tilde{\mathbf{h}}_m\}_{m=1}^M$ .

- A channel from the PTX to the SRX: A multipath channel from the PTX to the SRX is given by

$$\mathbf{f} = \mathbb{I}_L \sqrt{(d_2)^{-\epsilon_L}} \tilde{\mathbf{f}}_L + (1 - \mathbb{I}_L) \sqrt{(d_2)^{-\epsilon_{nL}}} \tilde{\mathbf{f}}_{nL} \quad (2)$$

where  $\tilde{\mathbf{f}}_L$  and  $\tilde{\mathbf{f}}_{nL}$  identify frequency selective fading channels over LoS and nLoS paths with  $N_L \triangleq \mathbb{L}(\tilde{\mathbf{f}}_L)$  and  $N_{nL} \triangleq \mathbb{L}(\tilde{\mathbf{f}}_{nL})$  multipath components. The path loss exponent over  $\mathbf{f}_{nL}$  is denoted by  $\epsilon_{nL}$ . The indicator function,  $\mathbb{I}_L$ , is used to model the random selection of LoS and nLoS paths with probability  $P_r(\mathbb{I}_L) = \mathcal{F}$  and  $P_r(\mathbb{I}_{nL}) = 1 - \mathcal{F}$  with time-sharing factor  $\mathcal{F}$  [18]. Owing to the random location of the PTX within the secondary users' network, we model it using a Bernoulli process. The distance  $d_2$  from the PTX to the SRX is distributed as follows:

$$f_{d_2}(y_2) = 2y_2/R^2 \text{ for } 0 \leq y_2 \leq R. \quad (3)$$

- Channels from the SU-RRHs to the PRX : When  $M$  SU-RRHs are available for dCDD, they influence the PRX, so that a channel from the  $m$ th SU-RRH to the PRX is given by

$$\mathbf{g}_m = \sqrt{(d_{3,m})^{-\epsilon_L}} \tilde{\mathbf{g}}_m \quad (4)$$

where  $\tilde{\mathbf{g}}_m$  identifies the frequency selective fading channel with  $N_g \triangleq \{\mathbb{L}(\tilde{\mathbf{g}}_m)\}_{m=1}^M$ . A specific distance from the  $m$ th RRH to the PRX is given by  $d_{3,m}$ .

- All frequency selective fading channels are assumed to be independent and identically distributed (i.i.d.). We also assume that all channels are constant over one data transmission interval due to a quasi-static channel assumption, but different from and independent of those for other transmission intervals.

#### A. dCDD for CP-SC Transmissions

As a transmission scheme, CP-SC transmissions [11]–[13] are used for the primary and secondary user networks. To remove ISI being caused by a multipath channel between two nodes, the last  $N_p$  modulation symbols from a transmission symbol block  $\mathbf{s} \in \mathbb{C}^{B \times 1}$  are appended to the front of  $\mathbf{s}$  [6]. The size of symbol block  $\mathbf{s}$  is denoted by  $B$ . We assume that  $E\{\mathbf{s}\} = \mathbf{0}$  and  $E\{\|\mathbf{s}\|^2\} = \mathbf{I}_B$ . To construct an ISI-free right circulant channel matrix, the CP length,  $N_p$ , and the CDD delay, for example,  $\Delta_m$  for the  $m$ th SU-RRH, play key roles in generating an equivalent ISI-free right circulant channel matrix by satisfying the following two conditions [6]:

$$N_p \geq N_h \text{ and } \Delta_m = (m-1)N_p. \quad (5)$$

Since CP-SC transmissions use block transmission, the maximum allowable number of SU-RRHs for dCDD is determined by  $K = 1 + \lfloor B/N_p \rfloor$ , where  $\lfloor \cdot \rfloor$  denotes the floor function. For dCDD, in this paper, we assume that only  $M \leq K$  SU-RRHs are available in the secondary users' network.

Due to dCDD, the received signal at the SRX, after removing the CP signal, is given by

$$\begin{aligned} \mathbf{r} = & \sqrt{P_s} \sum_{m=1}^M R^{-\epsilon_L/2} \tilde{\mathbf{H}}_m \tilde{\mathbf{s}}_m + \\ & \sqrt{P_P} (\mathbb{I}_{\text{L}} d_2^{-\epsilon_L/2} \tilde{\mathbf{F}}_{\text{L}} + (1 - \mathbb{I}_{\text{nL}}) d_2^{-\epsilon_L/2} \tilde{\mathbf{F}}_{\text{nL}}) \tilde{\mathbf{x}}_p + \mathbf{z}_R \end{aligned} \quad (6)$$

where  $\tilde{\mathbf{s}}_m \triangleq \mathbf{P}_B^{\Delta_m} \mathbf{s}_m$ ,  $P_P$  is the transmission power at the PTX. The permutation shifting matrix  $\mathbf{P}_B^{\Delta_m}$  is obtained from the identity matrix  $\mathbf{I}_B$  by circularly shifting down by  $\Delta_m$ . The transmission power at the SU-RRHs is  $P_s$ , which is given by the following constraint [13]:

$$P_s = \min \left( P_T, \frac{I_p}{\max_{m=1,\dots,M} P_G d_{3,m}^{-\epsilon_L} \|\tilde{\mathbf{g}}_m\|^2} \right) \quad (7)$$

where  $P_T$  and  $I_p$  respectively denote the maximum allowable transmission power at the SU-RRHs and the peak allowable interference at the PRX. The transmission power at the PRX is denoted by  $P_G$ . Channel matrices,  $\tilde{\mathbf{H}}_m$ ,  $\tilde{\mathbf{F}}_{\text{L}}$ , and  $\tilde{\mathbf{F}}_{\text{nL}}$  are right circulant respectively specified by  $\tilde{\mathbf{h}}_m$ ,  $\tilde{\mathbf{f}}_{\text{L}}$ , and  $\tilde{\mathbf{f}}_{\text{nL}}$ . Since  $\max\{N_h, N_{\text{L}}, N_{\text{nL}}, N_g\}$  is smaller than the block size  $B$ , zero padding is required in the representation of right circulant channel matrices. The transmission symbol block from the PTX is given by  $\mathbf{x}_p$  with  $E\{\mathbf{x}_p\} = \mathbf{0}$  and  $E\{\mathbf{x}_p \mathbf{x}_p^H\} = \mathbf{I}_B$ , and  $E\{\tilde{\mathbf{s}}_m \mathbf{x}_p^H\} = \mathbf{0}$ . The additive noise over the frequency selective fading channels is denoted by  $\mathbf{z}_R \sim \mathcal{CN}(\mathbf{0}, \sigma_z^2 \mathbf{I}_B)$ .

### III. PERFORMANCE ANALYSIS IN THE INTERFERENCE LIMITED REGION

From (6), the SIR measured at the SRX is given by

$$\begin{aligned} \gamma_{\text{SIR}} &\triangleq \frac{P_s \sum_{m=1}^M R^{-\epsilon_L} \|\tilde{\mathbf{h}}_m\|^2}{P_P (\mathcal{F} d_2^{-\epsilon_L} \|\tilde{\mathbf{f}}_{\text{L}}\|^2 + (1 - \mathcal{F}) d_2^{-\epsilon_{\text{nL}}} \|\tilde{\mathbf{f}}_{\text{nL}}\|^2)} \\ &= \min(P_T, I_p/X) Y \end{aligned} \quad (8)$$

where  $X \triangleq \max_{m=1,\dots,M} P_G d_{3,m}^{-\epsilon_L} \|\tilde{\mathbf{g}}_m\|^2$ ,  $Y \triangleq \frac{A}{B}$  with  $A \triangleq \sum_{m=1}^M R^{-\epsilon_L} \|\tilde{\mathbf{h}}_m\|^2$  and  $B \triangleq P_P (\mathcal{F} d_2^{-\epsilon_L} \|\tilde{\mathbf{f}}_{\text{L}}\|^2 + (1 - \mathcal{F}) d_2^{-\epsilon_{\text{nL}}} \|\tilde{\mathbf{f}}_{\text{nL}}\|^2)$ . Note that when we use the maximum likelihood type detector, for example, the QRD-M detector [21], we can obtain (8).

#### A. Distributions of the SA-SIR

Owing to the random location of the PTX within the secondary users' cell, we need to compute the SA-SIR. Extending from the analysis of [13], the CDF of the SA-SIR is given by

$$\begin{aligned} F_{\gamma}(x) = & \underbrace{\overbrace{F_Y(x/P_T|d_2)}^{J_1} F_X(\mu) +} \\ & \underbrace{\overbrace{E \left\{ \int_{\mu}^{\infty} F_Y(xt/I_p|d_2) dt \right\} f_X(t) dt}^{J_2}} \end{aligned} \quad (9)$$

where  $\mu \triangleq \frac{I_p}{P_T}$ . To compute (9), we can readily find the following distributions and density of RV  $X$ :

$$\begin{aligned} F_X(x) &= \prod_{m=1}^M \left( 1 - \frac{\Gamma_u(N_g, x/P_G d_{3,m}^{-\epsilon_L})}{\Gamma(N_g)} \right) \\ &= 1 + \Upsilon e^{-\tilde{\beta}x} x^{\tilde{l}}, \end{aligned} \quad (10)$$

$$f_X(x) = \Upsilon [\tilde{l} e^{-\tilde{\beta}x} x^{\tilde{l}-1} - \tilde{\beta} e^{-\tilde{\beta}x} x^{\tilde{l}}], \quad (11)$$

where  $\Gamma(\cdot)$  and  $\Gamma_u(\cdot)$  respectively denote the complete gamma function and upper incomplete gamma function. In addition,  $\tilde{\beta} \triangleq \sum_{t=1}^m \frac{1}{P_G d_{3,t}^{-\epsilon_L}}$ ,  $\tilde{l} \triangleq \sum_{t=1}^m \ell_t$ , and

$$\Upsilon \triangleq \sum_{m=1}^M (-1)^m \sum_{q_1=1}^{M-m+1} \cdots \sum_{q_m=q_{m-1}+1}^M \sum_{\ell_1=0}^{N_g-1} \cdots \sum_{\ell_m=0}^{N_g-1} \prod_{t=1}^m \left( \frac{1}{\ell_t! (P_G d_{3,q_t}^{-\epsilon_L})^{\ell_t}} \right). \quad (12)$$

According to the analysis provided in [6], the distribution of RV  $A$ , is given by

$$F_A(x) = 1 - \frac{\Gamma_u(MN_h, x/P_s R^{-\epsilon_L})}{\Gamma(MN_h)}. \quad (13)$$

Furthermore, from CP-SC transmissions, the conditional density of the primary user's interference power received at the SRX at a given distance  $d_2$ , denoted by an RV  $C$ , is given by

$$\begin{aligned} f_C(x|d_2) = & \frac{\mathcal{F}}{\Gamma(N_{\text{L}})(P_P d_2^{-\epsilon_L})^{N_{\text{L}}}} x^{N_{\text{L}}-1} e^{-\frac{x}{P_P d_2^{-\epsilon_L}}} + \\ & \frac{(1 - \mathcal{F})}{\Gamma(N_{\text{nL}})(P_P d_2^{-\epsilon_{\text{nL}}})^{N_{\text{nL}}}} x^{N_{\text{nL}}-1} e^{-\frac{x}{P_P d_2^{-\epsilon_{\text{nL}}}}} \end{aligned} \quad (14)$$

$$J_1 = 1 - \frac{2\mathcal{F}\rho^{-N_L}}{\epsilon_L \Gamma(N_L)} \left( \frac{x}{P_T} \right)^{-N_L} \sum_{m=0}^{MN_h-1} \frac{1}{m!} G_{2,2}^{2,1} \left( \frac{x\rho}{P_T} \mid \begin{array}{c} 1, N_L + 2/\epsilon_L + 1 \\ N_L + 2/\epsilon_L, N_L + m \end{array} \right) - \\ \frac{2(1-\mathcal{F})\rho^{-N_{nL}} R^{N_{nL}(\epsilon_{nL}-\epsilon_L)}}{\epsilon_{nL} \Gamma(N_{nL})} \left( \frac{x}{P_T} \right)^{-N_{nL}} \sum_{m=0}^{MN_h-1} \frac{1}{m!} G_{2,2}^{2,1} \left( \frac{x\rho R^{\epsilon_L - \epsilon_{nL}}}{P_T} \mid \begin{array}{c} 1, N_{nL} + 2/\epsilon_{nL} + 1 \\ N_{nL} + 2/\epsilon_{nL}, N_{nL} + m \end{array} \right). \quad (15)$$

with the density of  $d_2$  given by  $f_{d_2}(y_2) = \frac{2y_2}{R^2}$ ,  $0 \leq y_2 \leq R$ .

After having some manipulations, the expression for  $J_1$  in (9) can be evaluated as (15) at the top of this page. In (15), we have defined  $\rho \triangleq \frac{P_p}{P_s}$ . In addition,  $G_{p,q}^{m,n}(\cdot | \cdot; \cdot)$  denotes the Meijer-G functions [22, sec. (2.24)]. Due to space limitations, we omit the derivation of (15).

A more challenging task is the computation of  $J_2$  in (9). Since the integral solution of  $J_2$  in (9) does not exist, we apply an approximation in the asymptotic region provided in the following theorem.

*Theorem 1:* The approximate expression for  $J_2$  in the asymptotic region is given by (16) at the top of the next page.

*Proof:* According to [23], we first approximate the following Meijer-G function as

$$G_{2,2}^{2,1} \left( x \mid \begin{array}{c} 1, N_L + 2/\epsilon_L + 1 \\ N_L + 2/\epsilon_L, N_L + m \end{array} \right) x \rightarrow 0 \approx \frac{\Gamma(m - 2/\epsilon_L) \Gamma(N_L + 2/\epsilon_L) + x^{N_L+m} \Gamma(m + N_L)}{\Gamma(2/\epsilon_L + 1 - m)}. \quad (17)$$

And then after conducting some manipulations, we can derive (16). Note that since we can readily extract expressions for  $C_1, C_2, D_1$ , and  $D_2$ , we do not provide their corresponding expressions. ■

### B. Outage Probability

Using (15) and (16), the approximate outage probability at a given SIR threshold  $O_{th}$ , is given by (18) near the top of the next page.

### C. Asymptotic Diversity Gain Analysis

Using (17), we can approximate  $J_1$  as in (19) near the top of the next page, where we have used the approach provided in [23] for an asymptotic approximation of (a). Similarly,  $C_1, C_2, D_1$  and  $D_2$  are approximately proportional to  $(x/I_p)^{N_h M}$ . Thus, as  $P_T \rightarrow \infty$  and  $I_p \rightarrow \infty$ , while maintaining  $\mu$  a constant, the maximum diversity gain,  $G_d = MN_h$ , can be achieved by the use of dCDD in the secondary users' network. Thus, we can see that a different time sharing on LoS and nLoS paths, and primary users' system and channel parameters have no effect on the diversity gain.

## IV. SIMULATIONS

The following simulation setting is considered:

- $B = 192$  and  $N_p = 64$ , so that  $K = 3$  is the maximum number of the RRHs for dCDD.
- Quadrature phase-shift keying (QPSK) modulation is used.
- The path-loss exponents are assumed to be  $\epsilon_1 = 2.09$ ,  $\epsilon_2 = 3.75$ , and  $\epsilon_3 = 3.75$  in the considered system [17].

- The SRX is placed at the center of a disk-shaped secondary users' communication cell of radius  $R$ , within which the PRX is placed at  $(\Delta_x, \Delta_y)$ .
- Three SU-RRHs are placed at  $R^{j\pi/2}$ ,  $R^{j(\pi/2-\pi/10)}$ , and  $R^{j(\pi/2+\pi/10)}$ .

The curves obtained via link-level simulations are denoted by **Ex**. Analytical performance curves are denoted by **An**. The SIR threshold causing an outage is fixed at  $O_{th} = 1$  dB.

### A. Outage Probability Analysis

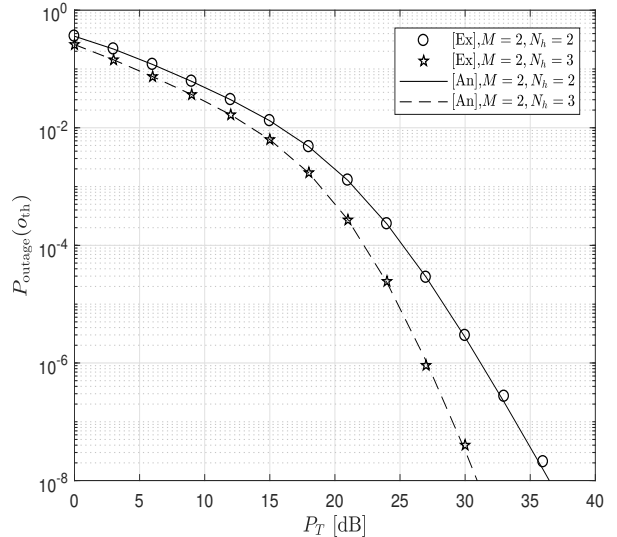


Fig. 2. Outage probability for various values of  $N_h$ .

Fig. 2 shows the outage probability for various values of  $N_h$  at fixed values of ( $M = 2, N_L = 2, N_{nL} = 3, N_g = 2, R = 10, \mathcal{F} = 0.6, P_p = 3$  dB,  $P_s = 1$  dB,  $P_g = 1$  dB,  $\Delta_x = 1, \Delta_y = 3$ ). This figure shows the accuracy of our derivations for the outage probability. Thus, in the sequel, we will mainly use the analytically derived outage probability for the performance analysis w.l.o.g..

Fig. 3 compares the outage probability of the proposed system with that of an existing scheme (denoted by conv. in the curves), which does not use dCDD. Only one SU-RRH, which has the largest SIR among them, is selected [3]–[5], [12], [13]. This figure shows that dCDD results in a better outage probability even with a small number of SU-RRHs in the secondary users' network. As more RRHs are available for dCDD, the performance gap will be increased. If we measure the slopes of the curves in this figure, they are identical when  $MN_h$  is same. This will be further investigated in Fig. 4.

In Fig. 4, we investigate different values for  $N_h$ ,  $\mathcal{F}$ ,  $R$ , and  $(N_L, N_{nL})$ . In the considered all cases, dCDD provides a

$$\begin{aligned}
J_2 &= 1 - F_X(\mu) - \frac{2\mathcal{F}\Upsilon\tilde{l}}{\epsilon_L\Gamma(N_L)} \sum_{m=0}^{MN_h-1} \frac{1}{m!} \left( \left( \frac{\rho x}{I_p} \right)^{2/\epsilon_L} \Gamma(m-2/\epsilon_L)\Gamma(N_L+2/\epsilon_L)(\tilde{\beta})^{-\tilde{l}-2/\epsilon_L} \Gamma_u(\tilde{l}+2/\epsilon_L, \tilde{\beta}\mu) + \right. \\
&\quad \left( \frac{\rho x}{I_p} \right)^m \Gamma(2/\epsilon_L+1-m)\Gamma(N_L+m)(\tilde{\beta})^{-\tilde{l}-m} \Gamma_u(\tilde{l}+m, \tilde{\beta}\mu) \right) + \\
&\quad \frac{2\mathcal{F}\Upsilon\tilde{\beta}}{\epsilon_L\Gamma(N_L)} \sum_{m=0}^{MN_h-1} \frac{1}{m!} \left( \left( \frac{\rho x}{I_p} \right)^{2/\epsilon_L} \Gamma(m-2/\epsilon_L)\Gamma(N_L+2/\epsilon_L)(\tilde{\beta})^{-\tilde{l}-2/\epsilon_L-1} \Gamma_u(\tilde{l}+2/\epsilon_L+1, \tilde{\beta}\mu) + \right. \\
&\quad \left( \frac{\rho x}{I_p} \right)^m \Gamma(2/\epsilon_L+1-m)\Gamma(N_L+m)(\tilde{\beta})^{-\tilde{l}-m-1} \Gamma_u(\tilde{l}+m+1, \tilde{\beta}\mu) \right) - \\
&\quad \frac{2(1-\mathcal{F})\Upsilon\tilde{l}}{\epsilon_L\Gamma(N_L)} \sum_{m=0}^{MN_h-1} \frac{1}{m!} \left( \left( \frac{\rho x R^{\epsilon_L-\epsilon_{nL}}}{I_p} \right)^{2/\epsilon_L} \Gamma(m-2/\epsilon_L)\Gamma(N_L+2/\epsilon_L)(\tilde{\beta})^{-\tilde{l}-2/\epsilon_L} \Gamma_u(\tilde{l}+2/\epsilon_L, \tilde{\beta}\mu) + \right. \\
&\quad \left( \frac{\rho x R^{\epsilon_L-\epsilon_{nL}}}{I_p} \right)^m \Gamma(2/\epsilon_L+1-m)\Gamma(N_L+m)(\tilde{\beta})^{-\tilde{l}-m} \Gamma_u(\tilde{l}+m, \tilde{\beta}\mu) \right) + \\
&\quad \frac{2(1-\mathcal{F})\Upsilon\tilde{\beta}}{\epsilon_L\Gamma(N_L)} \sum_{m=0}^{MN_h-1} \frac{1}{m!} \left( \left( \frac{\rho x R^{\epsilon_L-\epsilon_{nL}}}{I_p} \right)^{2/\epsilon_L} \Gamma(m-2/\epsilon_L)\Gamma(N_L+2/\epsilon_L)(\tilde{\beta})^{-\tilde{l}-2/\epsilon_L-1} \Gamma_u(\tilde{l}+2/\epsilon_L+1, \tilde{\beta}\mu) + \right. \\
&\quad \left( \frac{\rho x R^{\epsilon_L-\epsilon_{nL}}}{I_p} \right)^m \Gamma(2/\epsilon_L+1-m)\Gamma(N_L+m)(\tilde{\beta})^{-\tilde{l}-m-1} \Gamma_u(\tilde{l}+m+1, \tilde{\beta}\mu) \right) \\
&\stackrel{\triangle}{=} 1 - F_X(\mu) - C_1 + C_2 - D_1 + D_2. \tag{16}
\end{aligned}$$

$$\begin{aligned}
P_{\text{outage}}(O_{\text{th}}) &= 1 - F_X(\mu) \frac{2\mathcal{F}\rho^{-N_L}}{\epsilon_L\Gamma(N_L)} \left( \frac{O_{\text{th}}}{P_T} \right)^{-N_L} \sum_{m=0}^{MN_h-1} \frac{1}{m!} G_{2,2}^{2,1} \left( \frac{O_{\text{th}}\rho}{P_T} \mid \begin{array}{l} 1, N_L+2/\epsilon_L+1 \\ N_L+2/\epsilon_L, N_L+m \end{array} \right) - \\
&\quad F_X(\mu) \frac{2(1-\mathcal{F})\rho^{-N_{nL}}R^{N_{nL}(\epsilon_{nL}-\epsilon_L)}}{\epsilon_{nL}\Gamma(N_{nL})} \left( \frac{O_{\text{th}}}{P_T} \right)^{-N_{nL}} \sum_{m=0}^{MN_h-1} \frac{1}{m!} G_{2,2}^{2,1} \left( \frac{O_{\text{th}}\rho R^{\epsilon_L-\epsilon_{nL}}}{P_T} \mid \begin{array}{l} 1, N_{nL}+2/\epsilon_{nL}+1 \\ N_{nL}+2/\epsilon_{nL}, N_{nL}+m \end{array} \right) \\
&\quad - C_1 \Big|_{x=O_{\text{th}}} + C_2 \Big|_{x=O_{\text{th}}} - D_1 \Big|_{x=O_{\text{th}}} + D_2 \Big|_{x=O_{\text{th}}}. \tag{18}
\end{aligned}$$

$$\begin{aligned}
J_1 &\stackrel{P_T \rightarrow \infty}{\approx} 1 - \frac{2\mathcal{F}}{\epsilon_L\Gamma(N_L)} \sum_{m=0}^{MN_h-1} \left( \frac{\rho^{2/\epsilon_L}}{m!} \left( \frac{x}{P_T} \right)^{2/\epsilon_L} \Gamma(m-2/\epsilon_L)\Gamma(N_L+2/\epsilon_L) + \frac{\rho^m}{m!} \left( \frac{x}{P_T} \right)^m \Gamma(m+N_{nL}) \right. \\
&\quad \left. \Gamma(2/\epsilon_L+1-m) \right) - \frac{2(1-\mathcal{F})}{\epsilon_{nL}\Gamma(N_{nL})} \sum_{m=0}^{MN_h-1} \left( \frac{(\rho R^{\epsilon_L-\epsilon_{nL}})^{2/\epsilon_{nL}}}{m!} \left( \frac{x}{P_T} \right)^{2/\epsilon_{nL}} \Gamma(m-2/\epsilon_{nL}) \right. \\
&\quad \left. \Gamma(N_{nL}+2/\epsilon_{nL}) + \frac{(\rho R^{\epsilon_L-\epsilon_{nL}})^m}{m!} \left( \frac{x}{P_T} \right)^m \Gamma(m+N_{nL})\Gamma(2/\epsilon_{nL}+1-m) \right) \\
&\stackrel{(a)}{\approx} \left( \frac{x}{P_T} \right)^{N_h M}. \tag{19}
\end{aligned}$$

better outage probability over the conventional scheme. This figure also shows that

- As  $N_h$  increases, a better outage probability is obtained due to a higher multipath diversity gain.
- A different degree of co-existence of LoS and nLoS paths, which is specified by  $\mathcal{F}$ , does not influence the slope of the outage probability curve in the asymptotic region of  $P_T$ . Since we assume a constant  $\mu$ , this corresponds to an asymptotic region of  $I_p$  as well.
- A larger radius of the secondary users' communication cell, which is denoted by  $2R$ , affects adversely the outage probability due to a greater distance between SU-RRHs and the SRX.

- A different number of multipath components over the channel from the PTX to the SRX, does not change the slope of the outage probability curve in the asymptotic region, for example, ( $N_L = 2, N_{nL} = 3$ ) vs. ( $N_L = 5, N_{nL} = 6$ ) when  $MN_h$  is same.

## V. CONCLUSIONS

In this paper, we have investigated the performance enhancement of the secondary users for cooperative spectrum sharing systems. As the transmit diversity scheme, dCDD has been employed between the CU and distributed SU-RRHs. From the performance analysis, it has been seen that dCDD provides a better outage probability over an existing

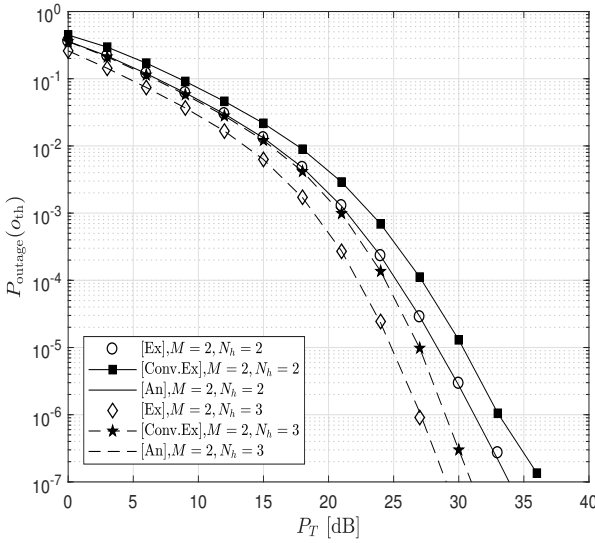


Fig. 3. Outage probability comparison with that of the existing work.

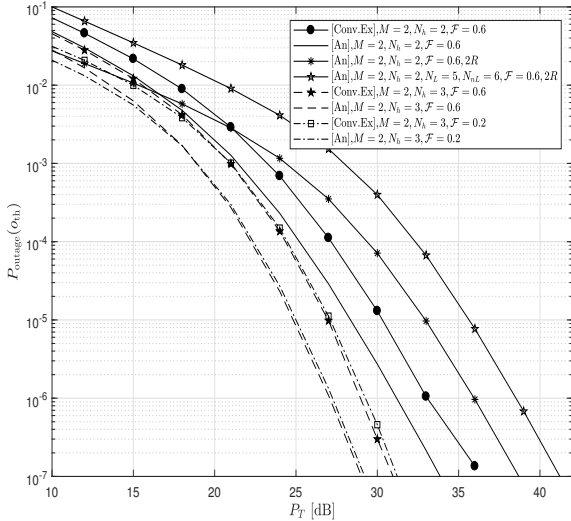


Fig. 4. Outage probability for various scenarios.

baseline system, which uses only one RRH as the secondary user transmitter. Furthermore, it has been justified from the simulations that the maximum diversity gain can be achieved. It has further been seen that the primary users' system and channel parameters have no impact on the achievable diversity gain of the secondary users' network.

## REFERENCES

- [1] T. K. Y. Lo, "Maximum ratio transmission," *IEEE Trans. Commun.*, vol. 47, no. 10, pp. 1458–1461, Oct. 1999.
- [2] K. J. Kim, T. Khan, and P. Orlik, "Performance analysis of cooperative systems with unreliable backhauls and selection combining," *IEEE Trans. Veh. Technol.*, vol. 66, no. 3, pp. 2448–2461, Mar. 2017.
- [3] V. M. Blagojevic and P. N. Ivanis, "Ergodic capacity for TAS/MRC spectrum sharing cognitive radio," *IEEE Commun. Lett.*, vol. 16, no. 3, pp. 312–323, Mar. 2012.
- [4] P. L. Yeoh, M. Elkashlan, T. Q. Trung, N. Yang, and D. B. da Costa, "Transmit antenna selection for interference management in cognitive relay networks," *IEEE Trans. Veh. Technol.*, vol. 63, no. 7, pp. 3250–3262, 2014.
- [5] M. Hanif, H. C. Yang, and M. S. Alouini, "Transmit antenna selection for power adaptive underlay cognitive radio with instantaneous interference constraint," *IEEE Trans. Commun.*, vol. 65, no. 6, pp. 2357–2367, Jun. 2017.
- [6] K. J. Kim, M. D. Renzo, H. Liu, P. V. Orlit, and H. V. Poor, "Performance analysis of distributed single carrier systems with distributed cyclic delay diversity," *IEEE Trans. Commun.*, vol. 65, no. 12, pp. 5514–5528, Dec. 2017.
- [7] Y.-C. Liang, W. S. Leon, Y. Zeng, and C. Xu, "Design of cyclic delay diversity for single carrier cyclic prefix (SCCP) transmissions with block-iterative GDFE (BI-GDFE) receiver," *IEEE Trans. Wireless Commun.*, vol. 7, no. 2, pp. 677–684, Feb. 2008.
- [8] A. H. Mehana and A. Nosratinia, "Single-carrier frequency-domain equalizer with multi-antenna transmit diversity," *IEEE Trans. Wireless Commun.*, vol. 12, pp. 388–397, Jan. 2013.
- [9] Q. Li, Q. Yan, K. C. Keh, K. H. Li, and Y. Hu, "A multi-relay-selection scheme with cyclic delay diversity," *IEEE Commun. Lett.*, vol. 17, no. 2, pp. 349–352, Feb. 2013.
- [10] U.-K. Kwon and G.-H. Im, "Cyclic delay diversity with frequency domain Turbo equalization for uplink fast fading channels," *IEEE Commun. Lett.*, vol. 13, no. 3, pp. 184–186, Mar. 2009.
- [11] K. J. Kim, T. A. Tsiftsis, and H. V. Poor, "Power allocation in cyclic prefixed single-carrier relaying systems," *IEEE Trans. Wireless Commun.*, vol. 10, no. 7, pp. 2297–2305, Jul. 2011.
- [12] K. J. Kim, T. Q. Duong, and H. V. Poor, "Outage probability of single-carrier cooperative spectrum sharing systems with decode-and-forward relaying and selection combining," *IEEE Trans. Wireless Commun.*, vol. 12, no. 2, pp. 806–817, Feb. 2013.
- [13] K. J. Kim, L. Wang, T. Q. Duong, M. Elkashlan, and H. V. Poor, "Cognitive single-carrier systems: Joint impact of multiple licensed transceivers," *IEEE Trans. Wireless Commun.*, vol. 13, no. 12, pp. 6741–6755, Dec. 2014.
- [14] X. Zhang and J. G. Andrew, "Downlink cellular network analysis with multi-slope path loss models," *IEEE Trans. Commun.*, vol. 63, no. 5, pp. 1881–1894, May 2015.
- [15] T. Bai, R. Vaze, and R. W. Heath, "Analysis of blockage effects on urban cellular networks," *IEEE Trans. Wireless Commun.*, vol. 9, no. 13, pp. 5070–5083, Sep. 2014.
- [16] M. Ding, P. Wang, D. Lopez-Perez, G. Mao, and Z. Lin, "Performance impact of LoS and NLoS transmissions in dense cellular networks," *IEEE Trans. Wireless Commun.*, vol. 15, no. 3, pp. 2365–2380, Mar. 2016.
- [17] 3GPP, TR 36.828 (V11.0.0), "Further enhancements to lte time division duplex (TDD) for downlink-uplink (DL-UL) interference management and traffic adaptation," Jun. 2012.
- [18] C. M. Lo and W. H. Lam, "Performance of generalized selection combining for mobile radio communications with mixed cochannel interferers," *IEEE Trans. Veh. Technol.*, vol. 51, no. 1, pp. 114–121, Jan. 2002.
- [19] Y. Zeng and T. S. Ng, "Pilot cyclic prefixed single carrier communication: channel estimation and equalization," *IEEE Signal Process. Lett.*, vol. 12, no. 1, pp. 56–59, Jan. 2005.
- [20] F. Gao, A. Nallanathan, and C. Tellambura, "Blind channel estimation for cyclic-prefixed single-carrier systems by exploiting real symbol characteristics," *IEEE Trans. Veh. Technol.*, vol. 56, no. 5, pp. 2487–2498, Sept. 2007.
- [21] K. J. Kim, Y. Yue, R. A. Iltis, and J. D. Gibson, "A QRD-M/Kalman Filter-based detection and channel estimation algorithm for MIMO-OFDM systems," *IEEE Trans. Wireless Commun.*, vol. 4, pp. 710–721, Mar. 2005.
- [22] A. P. Prudnikov, Y. A. Brychkov, and O. I. Marichev, *Integral and Series. Vol. 3: More Special Functions*, 3rd ed. London: Gordon and Breach, 1992.
- [23] K. An, M. Lin, T. Liang, J. B. Wang, J. Wang, Y. Huang, and A. L. Swindlehurst, "Performance analysis of multi-antenna hybrid satellite-terrestrial relay networks in the presence of interference," *IEEE Trans. Wireless Commun.*, vol. 63, no. 11, pp. 4390–4404, Nov 2015.